

Molecular magnetic resonance imaging discloses endothelial activation after transient ischaemic attack

Aurélien Quenault,¹ Sara Martinez de Lizarrondo,¹ Olivier Etard,^{2,3} Maxime Gauberti,¹ Cyrille Orset,¹ Benoît Haelewyn,⁴ Helen C. Segal,⁵ Peter M. Rothwell,⁵ Denis Vivien,^{1,6,*} Emmanuel Touzé^{1,7,*} and Carine Ali¹

* These authors contributed equally to this work.

Abstract

About 20% of patients with ischaemic stroke have a preceding transient ischaemic attack, which is clinically defined as focal neurological symptoms of ischaemic origin resolving spontaneously. Failure to diagnose transient ischaemic attack is a wasted opportunity to prevent recurrent disabling stroke. Unfortunately, diagnosis can be difficult, due to numerous mimics, and to the absence of a specific test. New diagnostic tools are thus needed, in particular for radiologically silent cases, which correspond to the recommended tissue-based definition of transient ischaemic attack. As endothelial activation is a hallmark of cerebrovascular events, we postulated that this may also be true for transient ischaemic attack, and that it would be clinically relevant to develop non-invasive *in vivo* imaging to detect this endothelial activation. Using transcriptional and immunohistological analyses for adhesion molecules in a mouse model, we identified brain endothelial P-selectin as a potential biomarker for transient ischaemic attack. We thus developed ultra-sensitive molecular magnetic resonance imaging using antibody-based microparticles of iron oxide targeting P-selectin. This highly sensitive imaging strategy unmasked activated endothelial cells after experimental transient ischaemic attack and allowed discriminating transient ischaemic attack from epilepsy and migraine, two important transient ischaemic attack mimics. We provide preclinical evidence that combining conventional magnetic resonance imaging with molecular magnetic resonance imaging targeting P-selectin might aid in the diagnosis of transient ischaemic attack.

Abbreviations: MCA(O) = middle cerebral artery (occlusion); MPIO = microparticle of iron oxide; SEP = somatosensory evoked potential; TIA = transient ischaemic attack; VWF = von Willebrand factor

Introduction

Worldwide, stroke is the second cause of death and a leading cause of disability. As the population ages, stroke is predicted to cause 8 million deaths in 2030 (Strong *et al.*, 2007). Despite advances in the acute treatment of stroke, prevention remains the most effective way to reduce this burden.

About 20% of patients with ischaemic stroke have a preceding transient ischaemic attack (TIA). Large cohort studies have demonstrated that TIA confers substantial short- and long-term risks of stroke, vascular events, myocardial infarction, cognitive impairment, and even death (Touzé *et al.*, 2005; Giles and Rothwell, 2007; Sivakumar *et al.*, 2014). Thus, TIA is a ‘warning’ event that provides an opportunity for prevention, and new guidelines highlight the need for urgent assessment of those patients.

TIA was originally defined as a sudden onset of a neurologic dysfunction lasting less than 24 h, presumably resulting from focal cerebral ischaemia. Recent guidelines proposed a tissue-based definition, in which TIA is a transient episode of neurological dysfunction caused by focal ischaemia, without acute infarction (Easton *et al.*, 2009). These radiologically silent TIAs account for 20–50% of all time-defined TIAs. In practice, diagnosis of TIA remains challenging, and many differential diagnoses exist (TIA mimics, like migraines, seizures, or syncope; Nadarajan *et al.*, 2014). Despite intensive efforts, the search for diagnostic biomarkers of ischaemic stroke has to date failed. This challenge could prove even more difficult in a less severe context like TIA.

Experimental models might therefore prove helpful to identify TIA-specific signatures (such as biological markers).

Molecular imaging is an emerging field in the clinical practice, with encouraging developments for *in vivo* imaging of inflammation. We recently developed a new formulation of microsized particles of iron oxide (MPIO) targeted against VCAM1 to achieve ultra-sensitive molecular imaging of cerebrovascular inflammation in CNS disorders. This molecular MRI method reached unprecedented sensitivity and specificity to reveal endothelial cell activation in the brain with the possibility to reveal discrete and early stages of endothelium dysfunction (Montagne *et al.*, 2012; Gauberti *et al.*, 2013). Molecular imaging of cerebrovascular inflammation thus appears as an interesting target for TIA, as endothelial dysfunction is at the origin of this pathology.

Our first goal was thus to optimize and characterize a pre-clinical mouse model of TIA, with laser Doppler-controlled ischaemia induced by middle cerebral artery occlusion, neurological activity recorded via somatosensory evoked potentials (SEPs), and potential brain lesions investigated by MRI. We thus determined the threshold of duration of occlusion not leading to MRI-evidenced brain lesion, and used it as a TIA model. Our second goal was to identify by polymerase chain reaction (PCR) and immunohistochemistry potential cerebro-vascular inflammatory markers of TIA. Our final goal was to develop an MRI-based strategy selective for TIA, relying on the use of targeted MPIOs. Overall, we found that P-selectin targeted molecular MRI is suitable to non-invasively unmask the discrete endothelial responses to TIA.

Materials and methods

Animals

Experiments were performed on male Swiss mice (□37 g; CURB), in accordance with French laws (act no. 87–848; Ministère de l'Agriculture et de la Forêt) and European Communities Council Directives of November 24, 1986 (86/609/EEC) guidelines, and were approved by the local ethical committee (CENOMEXA). None of the experimental procedures induced mortality. Experiments were performed following the ARRIVE guidelines (www.nc3rs.org.uk), including randomization and blind analyses. For surgeries, mice were anaesthetized with isoflurane 5% and maintained under anaesthesia with 2% isoflurane in a 70%/30% gas mixture (N₂O/O₂). The rectal temperature was maintained at $37 \pm 0.5^{\circ}\text{C}$ throughout using a feedback-regulated heating system.

Surgical procedure for transient ischaemic attack/ischaemic stroke and monitoring

We modified former models of selective neuronal necrosis or ischaemic stroke (Orset *et al.*, 2007; Arsava *et al.*, 2009; Moranchio *et al.*, 2012). The bifurcation of distal middle cerebral artery (MCA) was exposed after a small craniotomy, preserving the dura. A blunted haematology micropipette (Hoecht; tip diameter: 250 μm) was applied with an angular approach (30°) via a micromanipulator to induce MCA occlusion (MCAO) of selected durations (Fig. 1A). Regional cerebral blood velocity was measured by laser Doppler flowmetry (Oxford Optonix). Sham surgery was performed by the same approach without compression. Permanent MCAO was performed by electro-coagulation. Analyses of brain lesion volumes (Fig. 1D) led us to select 15 min MCAO as the optimum compression time to reproduce TIA, as it strictly complies with our criterion of a systematic and total absence of lesion on conventional MRI.

MRI of brain lesions

Imaging was carried out on a Pharmascan 7 T/12 cm system using surface coils (Bruker; Gauberti *et al.*, 2013). T2-weighted images to visualize infarction were acquired using MSME sequences (multi-spin multi-echo): echo time/repetition time: 51 ms/2500 ms with a 70 mm x 70 mm x 500 mm spatial resolution. Vascular permeability was assessed on 2D-TOF (time-of-flight) angiograms (echo time/repetition time: 12 ms/7 ms) and haemorrhage on T2* imaging (echo time/repetition time: 7.7 ms/500 ms) was performed. Lesion size was measured 24 h post-surgery on T2-weighted images using ImageJ (v1.45 r, NIH). In a longitudinal study, diffusion-weighted images (DWI) were acquired using a standard spin echo imaging modified with a Stejskal-Tanner gradient scheme. Parameters were: echo time/repetition time 2500 ms/29 ms, matrix size of 192 x 192 giving an in plane

resolution of 100 x 78 μm , slice thickness of 0.75 mm, one direction diffusion gradient (in the frequency encoding direction) with a b-factor of 1000 s/mm^2 and one averaging.

Somatosensory evoked potentials

SEPs were recorded in anaesthetized TIA mice using a dedicated Keypoint system (Alpine biomed). The skin was retracted and a gold-plated ball electrode (Grass technologies) was placed over the right sensory cortex, 2 mm behind the bregma and 2 mm lateral to midline (Troncoso *et al.*, 2000). Subdermal needle electrodes were placed on the nose and on the back for reference and ground, respectively. Isoflurane was then reduced and N2O was replaced with medical air while checking the loss of withdrawal reflex. The SEP recording was then started and the left forepaw was stimulated using ring electrodes (intensity: 2 mA; duration: 0.2 ms; frequency: 2.7 Hz; sweep: 20). MCAO was started when stable cortical responses were obtained. SEPs were recorded every minute until total recovery of cortical responses. For analyses, we considered the first positive and negative (P1 and N1) waves.

Quantitative real-time polymerase chain reaction for vascular adhesion molecules

Reverse transcription and quantitative PCR were performed as previously described (Montagne *et al.*, 2012). Forward (F) and reverse (R) primers were: *Vcam1* (F) gaacccaacagaggcagag, (R) tgagcaggtcaggttcacag; P-selectin (*Se1p*) (F) ggcaagtgggaatga-taacc, (R) ccatagaagcctgggtagca; *Gapdh* (F) tgcgactcaacag-caactc, (R) atgtaggccatgaggtccac.

Results were computed as follows: relative mRNA expression = $E^{-(Ct \text{ of gene of interest})/E^{-(Ct \text{ of GAPDH})}$, where Ct is the threshold cycle value and E is efficiency.

Immunohistochemistry for vascular adhesion molecules

Brain sections were processed for immunohistochemistry as described previously (Gauberti *et al.*, 2013). Primary antibodies were goat anti-P-selectin (1:1000; AF737, R&D Systems), rat monoclonal anti-VCAM-1 [1:1000; A(429) from BD Bioscience] or rabbit anti-von Willebrand factor (VWF) (1:800; Dako). Primary antibodies were revealed using Fab'2 fragments of donkey anti-rat, goat, rabbit or mouse IgG linked to fluorescein isothiocyanate (FITC), tetramethylrhodamine (TRITC) or DyLight® 629 (1:600, Jackson ImmunoResearch). The number of VWF-, P-selectin- and VCAM1-positive vessels was quantified in the cortex on 12 consecutive sections (covering the area of the occlusion site, between bregma 1.18 and -0.7mm). The specificity of immunostainings was checked by showing the absence of staining when primary antibodies were omitted or by performing immunostainings with a rat anti-mouse IgG monoclonal antibody (1:1000, Jackson ImmunoResearch) revealed with a FITC-coupled donkey anti-rat antibody (1:600, Jackson ImmunoResearch) (Supplementary Fig. 1).

ELISA for soluble P-selectin

Sham, TIA or ischaemic stroke mice were blood sampled after 24 h [blood collected on buffered sodium citrate (0.129 mol/l, pH = 5.2) and centrifuged at 1500g for 15 min and at 12 000g for 2 min to collect platelet free plasmas]. Murine soluble P-selectin levels were quantified using the soluble P-selectin/ CD62P Quantikine® ELISA kit (R&D Systems).

Targeting-moiety conjugation to MPIOs and molecular imaging

MPIOs (diameter 1.08 μm) with p-toluenesulphonyl reactive surface groups (Invitrogen) were used for peptide conjugation (Montagne *et al.*, 2012). Purified polyclonal goat anti-mouse antibodies for P-selectin (R&D Systems, clone AF737), purified monoclonal rat anti-mouse antibodies for P-selectin (BD Biosciences, clone RB 40.34), purified monoclonal rat anti-mouse antibodies for VCAM1 (BD Biosciences, clone MVCAM A429) or control rat IgG (Jackson ImmunoResearch) were covalently conjugated to MPIOs in borate buffer with

ammonium sulphate (pH 9.5), by incubation at 37°C for 48 h. Forty micrograms of targeting molecule (i.e. of each antibody) were used for the coating of 1mg of reactive MPIOs. MPIOs were then washed in phosphate-buffered saline (PBS) containing 0.5% bovine serum albumin (BSA) at 4°C and incubated for 24 h at room temperature, to block the remaining active groups. MPIOs were rinsed in PBS (0.1% BSA) and stored at 4°C.

For contrast-enhanced MRI, a caudal catheter was placed and mice received intravenous injection of 2.0 mg Fe/kg of conjugated MPIOs (200 μ l). Imaging was begun immediately after and lasted 20min after particle administration. 3D T2*-weighted gradient echo imaging with flow compensation (spatial resolution of 70 μ m x 70 μ m x 70 μ m interpolated to an isotropic resolution of 70 μ m) with echo time/repetition time: 13.2 ms/200 ms and a flip angle of 21° was performed to visualize MPIOs (acquisition time: 20 min). All T2*-weighted images presented are minimum intensity projections of five consecutive slices (yielding a z-resolution of 350 μ m). Signal voids quantification on 3D T2*-weighted images using automatic triangle threshold in ImageJ software (v1.45 r) (Gauberti *et al.*, 2013). Results are presented as volume of MPIOs-induced signal void divided by the volume of the structure of interest (in per cent).

The quality of conjugated MPIOs was systematically checked in a naïve mouse, by stereotaxic injection of lipopoly-saccharide (1 μ g in 1 μ l) in the striatum (0.5 mm anterior, 2.0 mm lateral, -3 mm ventral to the bregma).

Transient ischaemic attack mimics

Epileptic seizures were induced in awake mice by intraperitoneal injection of kainate (Tocris; 30 mg/kg in saline, 300 μ l injected; Mulle *et al.*, 1998).

Migraine was induced in awake mice, by the intraperitoneal injection of nitroglycerin at 10 mg/kg (VWR; in saline, 200 μ l injected; Pradhan *et al.*, 2014). Nitroglycerin triggers migraine in humans, and induces migraine-like attacks in rodents, with hyperalgesia and conditioned place aversion (Pradhan *et al.*, 2014).

Molecular MRI was performed 24 h after inducing TIA mimics.

Statistics

Apart from ELISA studies, for which box-and-whisker plots are shown, data are presented as mean \pm SEM and statistical analyses were performed with the Mann-Whitney's U-test, using the Statview software. For ELISA, comparisons between groups were done using ANOVA procedures in SAS 9.3.

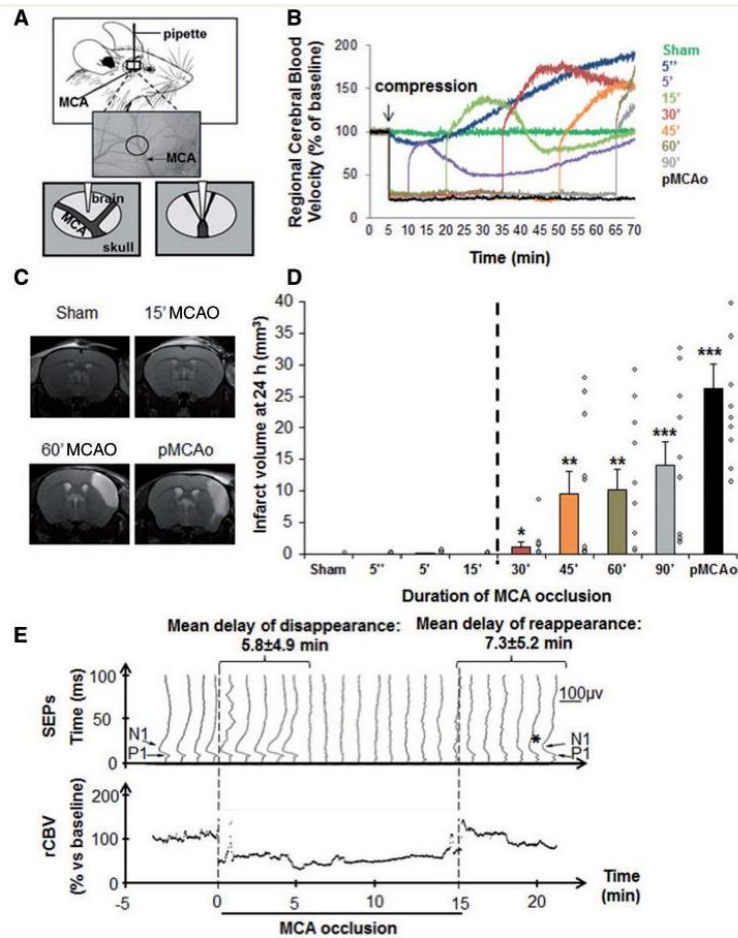


Figure 1 Vascular, radiological and neurological characterization of a preclinical mouse model corresponding to the tissue-based definition of TIA in humans. Compression-induced MCA occlusion leads to transient focal brain ischaemia. (A) Schematic description of the mouse model of TIA: after craniotomy, the parietal branch bifurcation of the MCA was exposed, without altering the integrity of the dura. An electrophysiology pipette was affixed and pushed to compress the MCA. (B) Compression-induced MCAO leads to transient focal brain ischaemia, as shown by regional cerebral blood velocity (rCBV) Doppler recordings (mean profiles of 10 mice per group). (C and D) A threshold of duration of MCAO distinguishes TIA from ischaemic stroke. (C) Representative T2 images 24 h after MCAO of different durations (0/sham, 15 or 60 min, and permanent occlusion). (D) Lesion volumes measured by MRI (hypersignals on T2) 24 h after MCAO of different durations. MCAO lasting up to 15 min, induced no brain lesions, while longer occlusions led to infarction that increased with the duration of ischaemia. Individual values are plotted as diamond shapes, and bars represent the mean volume lesion \pm standard error of the mean (SEM) ($n = 10$ per group, * $P < 0.05$, ** $P < 0.01$ and *** $P < 0.001$ versus sham). (E) Evidence of reversible functional deficits: P1 and N1 cortical waves were consistently recorded with a mean latency measured before occlusion of 11.2 ± 0.7 ms and 17.6 ± 2.0 ms, respectively, and a mean peak-to-peak amplitude of 77.2 ± 55.3 mV. The figure shows a horizontally stacked representative co-monitoring of regional cerebral blood velocity (continuous) and SEPs (every minute) for one representative mouse subjected to MCAO for 15 min. On the first curve, the P1 and N1 waves are highlighted. On this animal, P1 wave disappears 6 min after initiating MCAO and reappears (asterisk) 1 min after the end of occlusion, first inconstantly and then definitively 5 min after. The mean delays of disappearance and reappearance of SEPs relative to MCAO and MCA de-occlusion, respectively are reported on the top (mean \pm SEM; $n = 6$).

Results

Vascular adhesion molecules as putative biomarkers of transient ischaemic attack

We first optimized previous approaches to have a mouse model corresponding to the tissue-based definition of TIA (Fig. 1A). Doppler recordings (Fig. 1B and Supplementary Fig. 2) show that, regardless of the duration of compression, MCAO reproducibly induced a robust decrease in regional cerebral blood velocity of 75%. MCAO lasting longer than 15 min were associated with brain infarctions within 24 h, which volumes increased with the duration of MCAO (Fig. 1C, D and Supplementary Fig. 3A). Interestingly, for compressions lasting up to 15 min, no significant infarction was observed at the macro and microscopic levels, even after 3 months (Supplementary Fig. 3B and C). Yet, MCAO of 15 min of compression were sufficient to induce transient neurological deficits. Indeed, when looking at SEPs, the P1/N1 cortical complex had systematically disappeared 5.8 ± 4.9 min after initiation of MCAO. The functional dysfunction was transient, as the P1/N1 cortical complex reappeared in 7.3 ± 5.2 min after the release of the artery (Fig. 1E).

Based on these results, we considered that the model with MCAO for 15 min was a relevant model for the tissue-based definition of TIA: a vascular event with transient neurological disturbance, and no brain infarction on MRI.

Signs of inflammatory responses of the endothelium were then sought by RT-PCR for key cell adhesion molecules (VCAM1, ICAM1, E-selectin and P-selectin), 24 h after various durations of occlusion. *Vcam1* transcription is activated in both cortices, for MCAO longer than 45 min only, with a 2- to 3.5-fold increase in the ipsilateral versus contralateral cortex (Fig. 2A). By contrast, the expression of *Selp*/P-selectin, *Sele*/E-selectin and *Icam1* mRNA was activated in the ipsilateral cortex only, even for short MCAO, with differences between both cortices that could reach a factor 10 (Fig. 2A and data not shown). We then focused on VCAM1 and P-selectin. In immunohistological analyses, compared to control conditions, the proportion of VCAM1 and P-selectin-positive vessels in the MCA branch territory was increased after ischaemic stroke (13 and three times, respectively). Consistent with our mRNA study (Fig. 2A), while the expression of VCAM1 was unchanged following TIA, P-selectin levels were increased 3-fold versus controls (Fig. 2B and C). Neither VCAM1, nor P-selectin were detected in contralateral cortices (Supplementary Fig. 4). However, increased levels of P-selectin in relation with cerebrovascular insult could not be detected using circulating soluble P-selectin as a surrogate marker. Indeed in mouse plasmas, soluble P-selectin levels measured by ELISA tended to increase with the severity of the insult, but this was not significant (Supplementary Fig. 5). A small sample size study in the OXVASC population (Rothwell *et al.*, 2005) gave similar results (data not shown).

Combined T2-MRI with ultra-sensitive molecular MRI of P-selectin to positively diagnose transient ischaemic attack

We explored the possibility to directly detect brain P-selectin with targeted molecular imaging (Fig. 3A). Using the approach we used for VCAM1 (Montagne *et al.*, 2012; Gauberti *et al.*, 2013), we coupled MPIOs to a control immunoglobulin, or antibodies against P-selectin, AF737 and RB40.34. MPIOs were injected intravenously in mice 24 h after lipopolysaccharide injection in the striatum. In contrast to control IgG-coupled MPIOs, both P-selectin-targeted MPIOs induced ipsilateral hyposignals. The volume of signal void was 3-fold higher with AF737-MPIOs than with RB40.34-MPIOs (Fig. 3B and C). We thus selected AF737, and confirmed by *in vivo* optical imaging the interaction of AF737-MPIOs to the inflamed cerebrovasculature (Fig. 3D). Like MPIOs-oVCAM1 (Montagne *et al.*, 2012), the detachment of MPIOs-oP-selectin from the vasculature was 70% after 2 h and was almost complete after 24 h (Fig. 3E and F).

Mice subjected to sham surgery, TIA or ischaemic stroke, were subjected (24 h after injury) to a control magnetic resonance angiography (MRA)/T2/T2* MRI and then injected with MPIOs-oP-selectin or MPIOs-oVCAM1 for molecular imaging. After ischaemic stroke, there were hyposignals in the MCA territory, with both MPIOs-oVCAM1 (the ipsi- versus contralateral signal was doubled over sham mice) or MPIOs-oP-selectin (the ipsi- versus contralateral signal was 6.5-times higher than in sham mice) (Fig. 4A and B). After TIA, there was no difference with MPIOs-oVCAM-1 compared to sham animals. By contrast, the ipsi/contralateral signal

void with MPIOs-oP-selectin was 6.5-times higher in TIA versus sham animals (Fig. 4A and B). Interestingly, signal voids were 1.5-fold higher 6 h after TIA than in sham mice, reflecting the initiation of cerebrovascular inflammation. Forty-eight hours after TIA, signal voids with MPIOs-oP-selectin were lower than at 24 h, but remained 2.5-fold higher than in sham mice (not significant, but indicative of a persistent inflammation; Supplementary Fig. 6).

Finally, MPIOs-oP-selectin and MPIOs-oVCAM1 were tested 24 h after inducing two frequent TIA mimics, i.e. migraine and epilepsy. In epilepsy, MPIOs-oP-selectin imaging was also identical to that in sham animals, while MPIOs-oVCAM-1 signals were 15-times bigger in kainate-treated mice in the hippocampal area, as expected (Fig. 5A and B). In migraine, MPIOs-oP-selectin imaging was unaltered, whereas MPIOs-oVCAM-1 signals were increased by 140%, as expected, in the area of the trigeminal nucleus caudalis, but also in the cerebellum (Fig. 5C and D).

Together, these data show that molecular imaging for P-selectin in a context of transient neurological deficit without evidence of brain lesion by MRI could be used to diagnose TIA and discriminate it from migraine and epilepsy, two TIA mimics (Fig. 6).

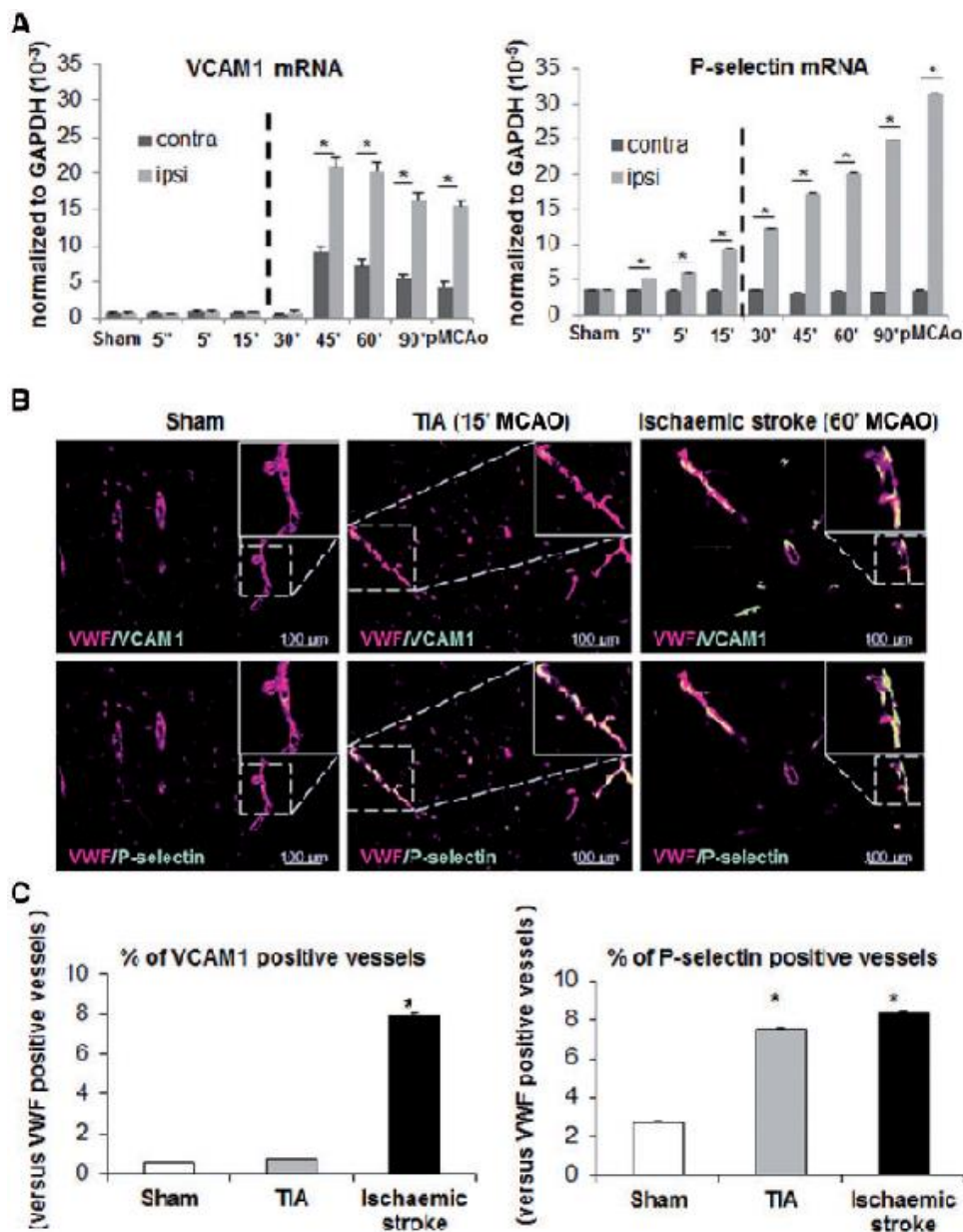


Figure 2 Vascular adhesion molecules as putative biomarkers to discriminate ischaemic stroke from TIA.

(A) RT-PCR analyses of mRNA cortical levels for Vcam1 and Selp (P-selectin), two key markers of endothelial activation 24 h after MCAO of different durations. Bars are mean values for expression in ipsilateral and contralateral cortices normalized to expression levels of Gapdh mRNA (n = 3 per group; *P50.05 versus sham). (B) Representative immunohistological images of slices stained with antibodies against VWF, P-selectin, VCAM1 in the cortex of sham, TIA and stroke mice and corresponding quantifications (C). A total of 5095, 5452 and 5537 VWF-positive vessels were counted on slices obtained from sham, TIA and ischaemic mice, respectively. The proportion of vessels co-stained with VWF and either P-selectin or VCAM1 was then calculated (*P50.05 versus sham, n = 3).

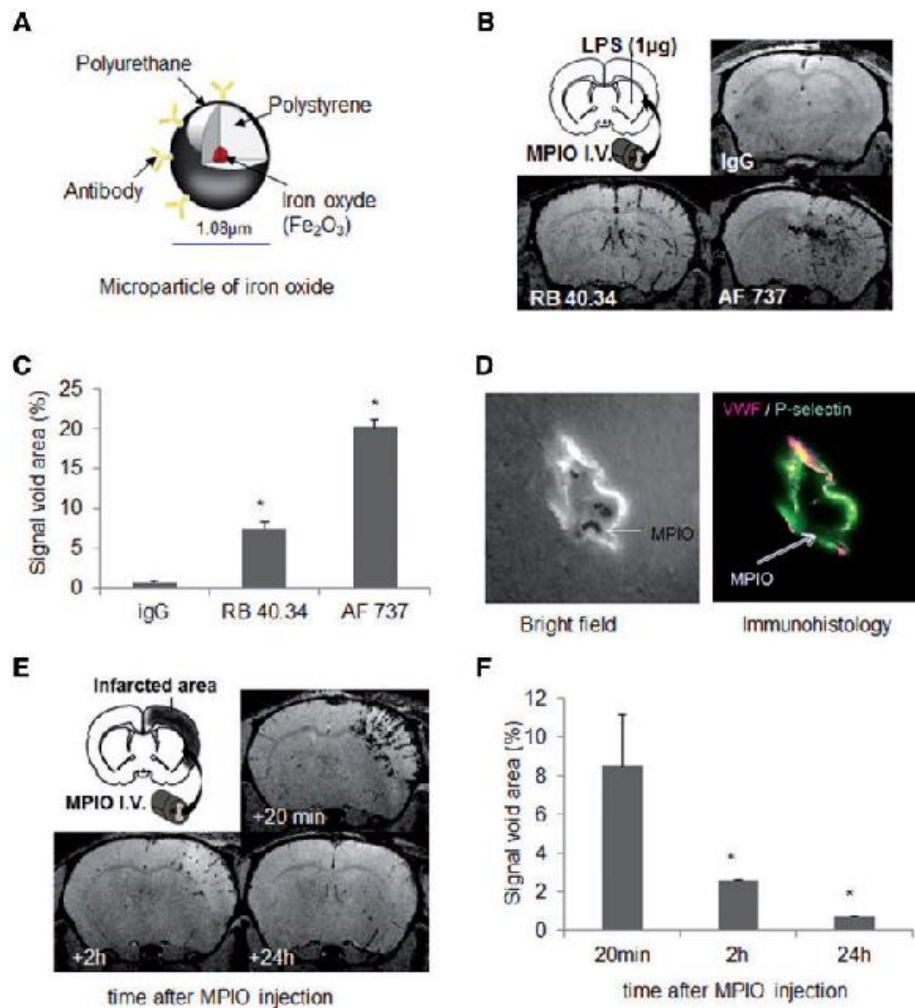


Figure 3 Development and optimization of MPIO-aP-selectin for ultrasensitive molecular MRI of cerebrovascular inflammation. (A) Schematic description of targeted MPIOs. (B and C) Stereotaxic injection of 1 mg of lipopolysaccharide (LPS) in striatum was performed in anaesthetized mice. Molecular MRI acquired 20 min after intravenous (I.V.) administration of targeted-MPIOs (24 h after lipopolysaccharide, $n = 3$ per group) showed signal voids corresponding to MPIOs binding. MPIO conjugate to IgG did not induce signal void. AF737-coupled MPIO revealed better contrast enhancement than RB40.34-coupled MPIO (* $P < 0.05$ versus sham). (D) Bright field and confocal imaging of a cerebral vessel immunostained with antibodies against VWF and P-selectin showed in vivo ability of targeted MPIOs to bind P-selectin at the endothelial surface. (E and F) Kinetics of AF737-coupled MPIO clearance from ischaemic stroke mice ($n = 3$) and corresponding quantification. Signal voids decreased gradually with time after MPIO-aP-selectin injection.

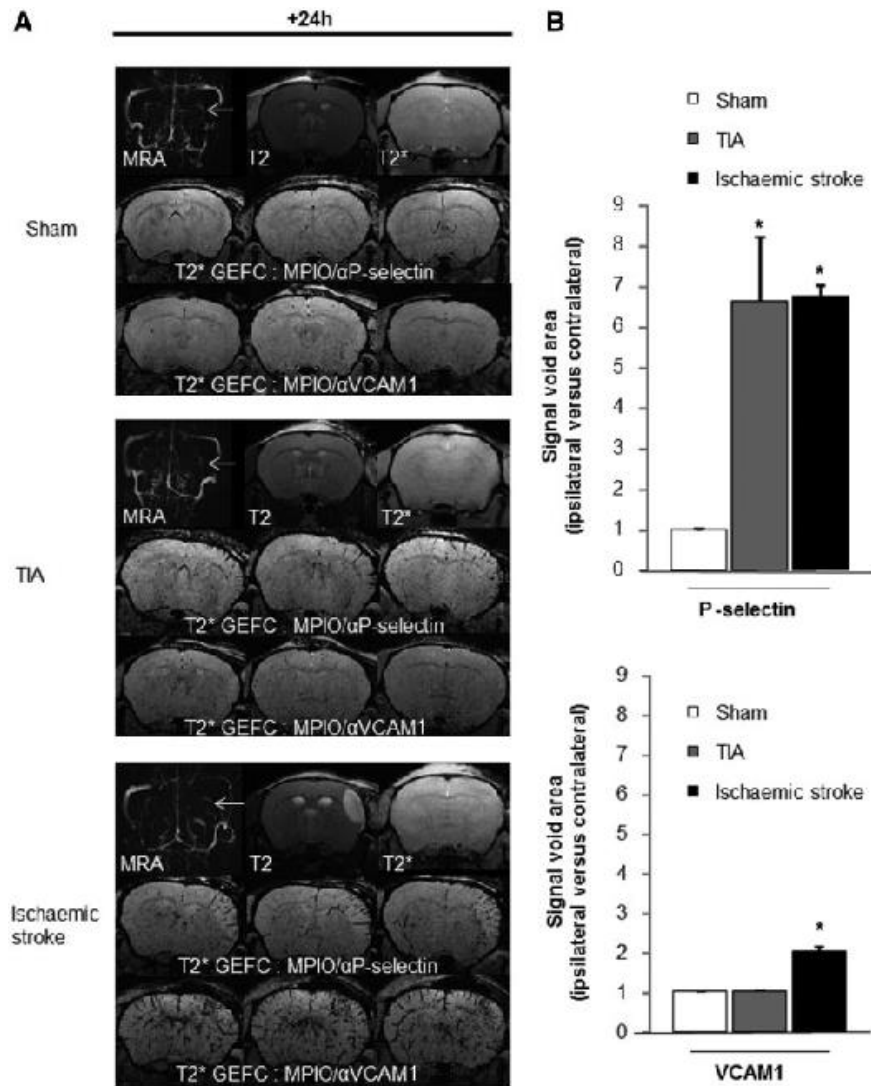


Figure 4 High resolution molecular MRI of P-selectin positively diagnoses TIA. (A) Representative MRA, T2 and T2* images and molecular imaging [serial T2* gradient echo imaging with flow compensation (GEFC) images] of P-selectin and VCAM1, 24 h post-surgery in sham, TIA and ischaemic stroke mice and corresponding quantifications (B) of signal void areas (ipsi/contralateral MCA territory; n = 5 per group; *P<0.05 versus sham).

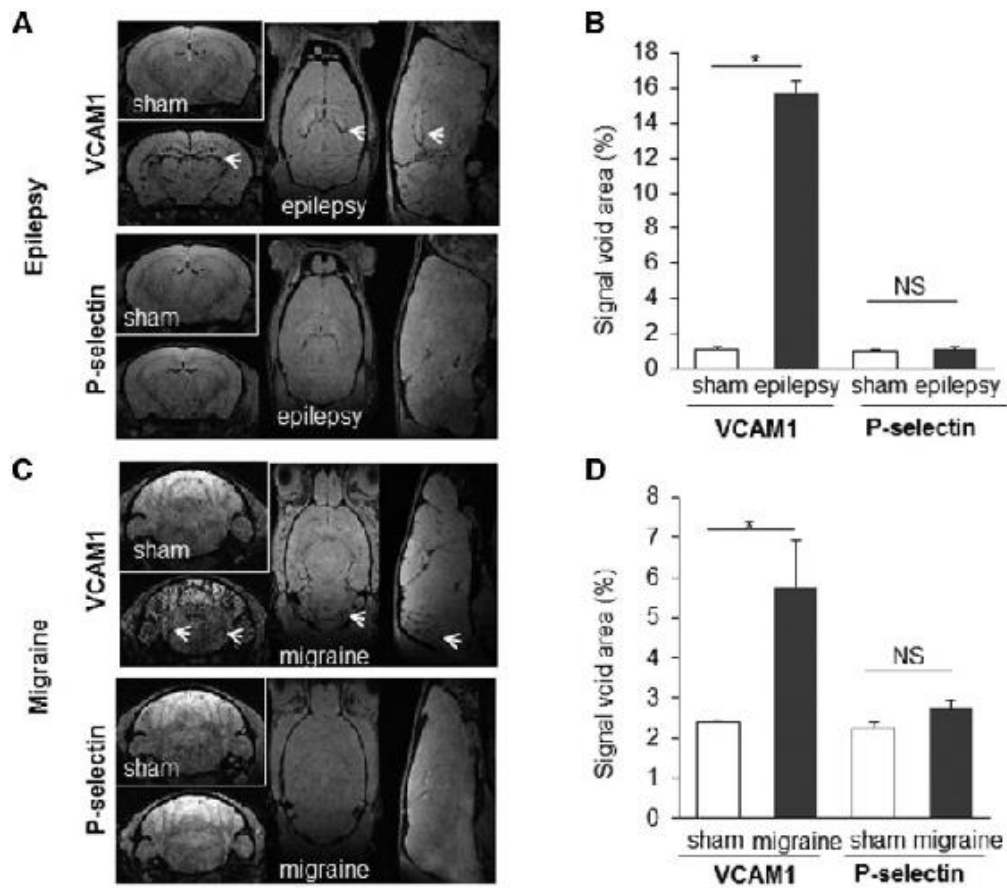


Figure 5 High resolution molecular MRI of P-selectin discriminates TIA from epilepsy and migraine, two TIA mimics. Representative images and corresponding quantifications of molecular MRI of P-selectin and VCAM1 in sham animals (saline) and 24 h after inducing epilepsy (kainate 30 mg/kg; intraperitoneally) (A and B) or migraine (nitroglycerin 10 mg/kg; intraperitoneally) (C and D) (n = 5 per group; *P<0.05 versus sham). Areas expected to be active in each condition are designated by an arrow: the hippocampus for epilepsy and the trigeminal nucleus for migraine.

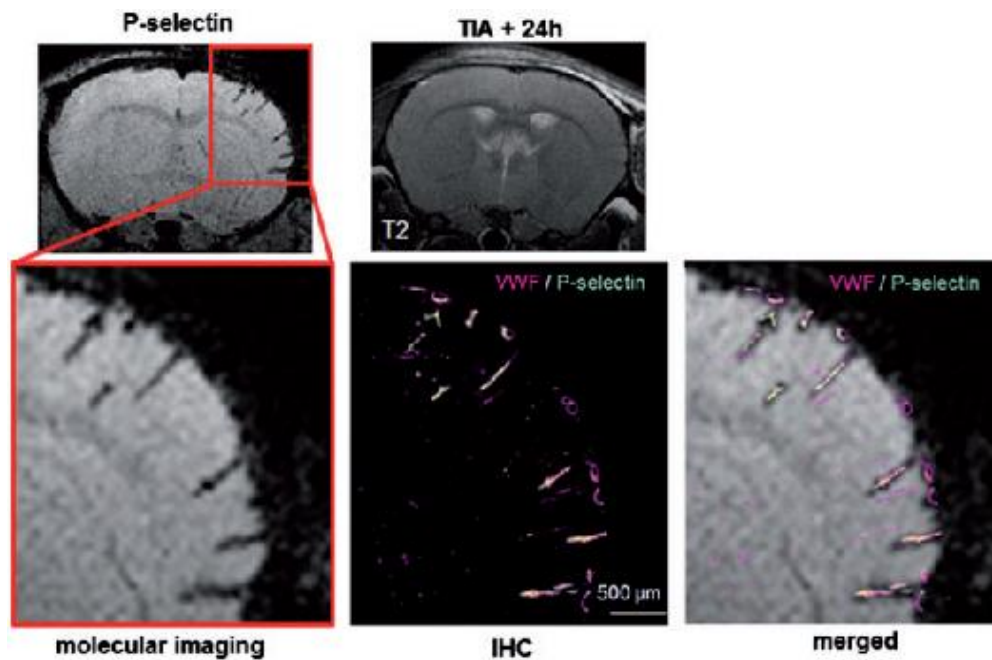


Figure 6 Illustration of the current state of TIA imaging in the clinical setting (i.e. no brain infarct on T2 or DWI images) and its potential future improvement evidencing a cerebrovascular inflammation revealed by molecular MRI of P-selectin. A superimposition of molecular MRI and regular immunostaining showed that MPIOs targeted for P-selectin are specific signals.

Discussion

TIA patients are at risk of adverse events, especially stroke, and must thus be managed appropriately. Although the risk of early stroke might be stratified by clinical scale and/or imaging modalities (Giles *et al.*, 2011), the lack of an objective and selective strategy to diagnose TIA limits appropriate preventive therapies (Rothwell *et al.*, 2007). In this study, we provided the proof-of-concept that molecular MRI of P-selectin could be used to positively diagnose TIA by disclosing endothelial activation.

Here, we first implemented and optimized previous models to establish a preclinical mouse model of TIA complying with the tissue-based definition. This model combines the advantages of these previous models (Fieschi *et al.*, 1975; Arsava *et al.*, 2009; Pedrono *et al.*, 2010; Moranco *et al.*, 2012; Ejaz *et al.*, 2015): it is relatively non-invasive, robust, reproducible, easy to control, and preserves the dura. The main achievement with this model is the supply of an MRI-based objective evidence of TIA.

Considering clinical observations reporting an activation of the peripheral immune system (Jickling *et al.*, 2012), we speculated that TIA could also initiate a cerebrovascular inflammatory response. Like previous studies, we found upregulated cortical levels of adhesion molecules after ischaemic stroke (Wang and Feuerstein, 1995; Berti *et al.*, 2002). After TIA, while VCAM1 was unaffected, P-selectin (and to a lesser extent ICAM1 and E-selectin) was upregulated. Transmigration of inflammatory cells is normally initiated by tethering/rolling and then firm adhesion along the endothelium, two processes involving P-selectin and VCAM1, respectively. In our TIA model, only P-selectin is detectable at the endothelial surface, while both P-selectin and VCAM1 are present in the stroke model. The underlying mechanism for this differential expression remains unestablished, but most likely results from the milder severity of the insult after a TIA (Lee *et al.*, 2004), not leading to the actual adhesion/diapedesis of inflammatory cells. Alternatively, it could reflect the activation of distinct pathways of inflammatory transmigration ultimately leading to the recruitment of distinct immune cell subsets (Battistini *et al.*, 2003).

As soluble P-selectin levels could not be used as a surrogate marker of cerebrovascular P-selectin, we chose an alternative *in vivo* detection strategy, i.e. molecular imaging of P-selectin. Imaging approaches to visualize brain-immune interactions are very attractive, in particular molecular MRI, which combines high spatial and temporal resolutions, as well as fast acquisition time (Jefferson *et al.*, 2012; Gauberti *et al.*, 2014). In the past, others have used MRI, PET or multispectral optoacoustic tomography, and targeted P-selectin by using labelled ligands (e.g. ^{68}Ga -Fucoidan) or by coupling contrast agents to ligands (e.g. fucoidan, antibodies, sialyl Lewis^X) (Jin *et al.*, 2009; McAteer *et al.*, 2012; Beziere *et al.*, 2014; Farr *et al.*, 2014; Li *et al.*, 2014). In a stroke/neuroinflammation context, P-selectin has been targeted in molecular MRI studies, with disappointing results: P-selectin targeted USPIOs (ultrasmall particles of iron oxide) had a limited sensitivity and specificity in a mouse ischaemic stroke model (Jin *et al.*, 2009) and a dual antibody-conjugated MPIOs, targeting both VCAM1 and P-selectin, did not show better images over single VCAM1 antibody-conjugated MPIOs in a model of acute inflammation in mice (McAteer *et al.*, 2012). More recently, sialyl Lewis^X-conjugated silica iron nanoparticles have been tested in a rodent stroke model. However, the contrast agent was not specific for P-selectin and did not give better results than control particles. Moreover, signals were reported equally increased throughout the brain (Farr *et al.*, 2014).

MPIOs offer important advantages for endothelial-targeted imaging (Jefferson *et al.*, 2012; Gauberti *et al.*, 2014). First, their micrometre size range allows endovascular specificity, since MPIOs are not taken-up by endothelial cells and do not passively diffuse in the brain parenchyma even with blood-brain barrier breakdown. Second, MPIOs have a very short blood half-life of 50–100 s (Ye *et al.*, 2008; Yang *et al.*, 2010), allowing imaging only MPIO binding to antigen immediately after injection. Third, MPIOs convey a large payload of iron oxide (usually 0.1–1.6 pg/particle), resulting in strong hypointense contrast effects that may extend up to 50 times the physical diameter of the particle. This phenomenon, known as the ‘blooming effect’, provides high sensitivity *in vivo* MRI detection, using only a small number of MPIO particles (Heyn *et al.*, 2006; Shapiro *et al.*, 2006).

Here, we took advantage of our recent improvements of MPIOs-aVCAM1-based imaging (Montagne *et al.*, 2012; Gauberti *et al.*, 2013) to develop high quality MPIOs-aP-selectin. In our mouse model, we demonstrated that MPIOs-aP-selectin can be used for a positive and selective MRI-based diagnosis of TIA (even in radiologically silent cases) and that this modality combined with T2 MRI can experimentally discriminate TIA from at least two major TIA mimics, migraine and epilepsy. The superposition between molecular MRI study and patterns of staining in immunohistological analyses of perfused brains support our hypothesis that molecular imaging signals reflect specific endothelial P-selectin (translocated from Weibel-Palade bodies to the surface upon activation, and refueled by neo-synthesis), even if we cannot exclude that, part of the signals could arise from adherent platelets. Noteworthy, unmasking an endothelial response after a very mild injury (15 min occlusion) demonstrates the sensitivity of our MRI-based approach.

Another interesting point is that positive signals with MPIOs-aP-selectin were evident on a relatively opened time-window (up to 48 h after TIA in our model). This observation first suggests that despite no evidence of macroscopic damage, TIA actually induces tissue sequelae, consistent with previous post-mortem histological findings (Ejaz *et al.*, 2015, 2016), but that our MRI modality non-invasively unmasks. Second, in the clinical setting, this time window gives a reasonable opportunity to process imaging, and to identify patients eligible for prevention.

Three characteristics of targeted MPIOs may limit their transfer for human applications (McAteer *et al.*, 2010; Gauberti *et al.*, 2014). First, due to their polyurethane coat, current MPIOs are non-biodegradable and may therefore accumulate in tissues, even for long periods (McAteer *et al.*, 2010; Roose *et al.*, 2014). However, development of new biodegradable coats is already ongoing (McAteer *et al.*, 2010; Gauberti *et al.*, 2014) and has even been tested in humans with new USPIOs like ferumoxytol (McBride *et al.*, 2015). Second, though iron toxicity could be questioned, the dose we used is in the range of that administered to humans for USPIO-based MRI of tumours, abdominal aortic aneurysms or ischaemic stroke (Saleh *et al.*, 2004; Will *et al.*, 2006; McBride *et al.*, 2015). No adverse effects had been reported in these studies. Third, the antibody carried by the MPIO might have a potential immunogenicity, but again, competitive ongoing strategies to increase the tolerance to

therapeutic or diagnostic antibodies (single chain or humanized antibodies, nanobodies) should overcome this limit. Thus, targeted molecular MRI really has a good chance of becoming a reference technic in the clinical setting.

Until now, finding a biomarker for TIA has remained challenging, not necessarily regarding the identification of a target, but rather, due to a limited sensitivity of techniques. Here, we propose that molecular MRI targeting P-selectin could increase the reliability of TIA diagnosis especially for patients with silent conventional MRI. Interestingly, this strategy not only provides sensitive and specific radiological evidence but also supports clinical conclusions, if reported neurological symptoms are consistent with the topography of the vascular territory with MPIOs signals. In conclusion, the proof-of-concept discovered in our preclinical models encourages future studies to investigate the specificity, sensitivity and feasibility of molecular MRI targeting P-selectin for the diagnosis of TIA.

Acknowledgment

We are grateful to Dr Benoit Roussel for his expertise in qPCR.

Funding

This work was funded by INSERM, Caen University and the Regional Council of Lower Normandy. The Oxford Vascular Study has been funded by the Wellcome Trust, Wolfson Foundation, UK Stroke Association, British Heart Foundation, Dunhill Medical Trust, National Institute of Health Research, Medical Research Council, and the NIHR Oxford Biomedical Research Centre.

Supplementary material

Supplementary material is available at *Brain* online.

References

1. Arsava EM, Gurer G, Gursoy-Ozdemir Y, Karatas H, Dalkara T. A new model of transient focal cerebral ischemia for inducing selective neuronal necrosis. *Brain Res Bull* 2009; 78: 226–31.
2. Battistini L, Piccio L, Rossi B, Bach S, Galgani S, Gasperini C, et al. CD8 + CD8 + T cells from patients with acute multiple sclerosis display selective increase of adhesiveness in brain venules: a critical role for P-selectin glycoprotein ligand-1. *Blood* 2003; 101: 4775–82. Berti R, Williams AJ, Moffett JR, Hale SL, Velarde LC, Elliott PJ, et al. Quantitative real-time RT-PCR analysis of inflammatory gene expression associated with ischemia-reperfusion brain injury. *J Cereb Blood Flow Metab* 2002; 22: 1068–79.
3. Beziere N, von Schacky C, Kosanke Y, Kimm M, Nunes A, Licha K, et al. Optoacoustic imaging and staging of inflammation in a murine model of arthritis. *Arthritis Rheumatol* 2014; 66: 2071–8.
4. Easton JD, Saver JL, Albers GW, Alberts MJ, Chaturvedi S, Feldmann E, et al. Definition and evaluation of transient ischemic attack: a scientific statement for healthcare professionals from the American Heart Association/American Stroke Association Stroke Council; Council on Cardiovascular Surgery and Anesthesia; Council on Cardiovascular Radiology and Intervention; Council on Cardiovascular Nursing; and the Interdisciplinary Council on Peripheral Vascular Disease. The American Academy of Neurology affirms the value of this statement as an educational tool for neurologists. *Stroke* 2009; 40: 2276–93.
5. Ejaz S, Emmrich JV, Sawiak SJ, Williamson DJ, Baron JC. Cortical selective neuronal loss, impaired behavior, and normal magnetic resonance imaging in a new rat model of true transient ischemic attacks. *Stroke* 2015; 46: 1084–92.
6. Ejaz S, Emmrich JV, Sitnikov SL, Hong YT, Sawiak SJ, Fryer TD, et al. Normobaric hyperoxia markedly reduces brain damage and sensorimotor deficits following brief focal ischaemia. *Brain* 2016; 139 (Pt 3): 751–64.

7. Farr TD, Lai CH, Grünstein D, Orts-Gil G, Wang CC, Boehm-Sturm P, et al. Imaging early endothelial inflammation following stroke by core shell silica superparamagnetic glyconanoparticles that target selectin. *NanoLett* 2014; 14: 2130–4.
8. Fieschi C, Battistini N, Volante F, Zanette E, Weber G, Passero S. Animal model of TIA: an experimental study with intracarotid ADP infusion in rabbits. *Stroke* 1975; 6: 617–21.
9. Gauberti M, Montagne A, Marcos-Contreras OA, Le Béhot A, Maubert E, Vivien D. Ultra-sensitive molecular MRI of vascular cell adhesion molecule-1 reveals a dynamic inflammatory penumbra after strokes. *Stroke* 2013; 44: 1988–96.
10. Gauberti M, Montagne A, Quenault A, Vivien D. Molecular magnetic resonance imaging of brain-immune interactions. *Front Cell Neurosci* 2014; 8: 389.
11. Giles MF, Rothwell PM. Risk of stroke early after transient ischaemic attack: a systematic review and meta-analysis. *Lancet Neurol* 2007; 6: 1063–72.
12. Giles MF, Albers GW, Amarenco P, Arsava EM, Asimos AW, Ay H, et al. Early stroke risk and ABCD2 score performance in tissue- vs time-defined TIA: a multicenter study. *Neurology* 2011; 77: 1222–8. Heyn C, Ronald JA, Mackenzie LT, MacDonald IC, Chambers AF, Rutt BK, et al. In vivo magnetic resonance imaging of single cells in mouse brain with optical validation. *Magn Reson Med* 2006; 55: 23–9.
13. Jefferson A, Wijesurendra RS, McAteer MA, Choudhury RP. Development and application of endothelium-targeted microparticles for molecular magnetic resonance imaging. *Wiley Interdiscip Rev Nanomed Nanobiotechnol* 2012; 4: 247–56.
14. Jickling GC, Zhan X, Stamova B, Ander BP, Tian Y, Liu D, et al. Ischemic transient neurological events identified by immune response to cerebral ischemia. *Stroke* 2012; 43: 1006–12.
15. Jin AY, Tuor UI, Rushforth D, Filfil R, Kaur J, Ni F, et al. Magnetic resonance molecular imaging of post-stroke neuroinflammation with a P-selectin targeted iron oxide nanoparticle. *Contrast Media Mol Imaging* 2009; 4: 305–11.
16. Lee YW, Eum SY, Nath A, Toborek M. Estrogen-mediated protection against HIV Tat protein-induced inflammatory pathways in human vascular endothelial cells. *Cardiovasc Res* 2004; 63: 139–48.
17. Li X, Bauer W, Israel I, Kreissl MC, Weirather J, Richter D, et al. Targeting P-selectin by gallium-68-labeled fucoidan positron emission tomography for noninvasive characterization of vulnerable plaques: correlation with in vivo 17.6T MRI. *Arterioscler Thromb Vasc Biol* 2014; 34: 1661–7.
18. McAteer MA, Akhtar AM, von Zur Muhlen C, Choudhury RP. An approach to molecular imaging of atherosclerosis, thrombosis, and vascular inflammation using microparticles of iron oxide. *Atherosclerosis* 2010; 209: 18–27.
19. McAteer MA, Mankia K, Ruparelia N, Jefferson A, Nugent HB, Stork LA, et al. A leukocyte-mimetic magnetic resonance imaging contrast agent homes rapidly to activated endothelium and tracks with atherosclerotic lesion macrophage content. *Arterioscler Thromb Vasc Biol* 2012; 32: 1427–35.
20. McBride OM, Berry C, Burns P, Chalmers RT, Doyle B, Forsythe R, et al. MRI using ultrasmall superparamagnetic particles of iron oxide in patients under surveillance for abdominal aortic aneurysms to predict rupture or surgical repair: MRI for abdominal aortic aneurysms to predict rupture or surgery-the MA(3)RS study. *Open Heart* 2015; 2: e000190.
21. Montagne A, Gauberti M, Macrez R, Jullienne A, Briens A, Raynaud JS, et al. Ultra-sensitive molecular MRI of cerebrovascular cell activation enables early detection of chronic central nervous system disorders. *Neuroimage* 2012; 63: 760–70.
22. Morancho A, García-Bonilla L, Barceló V, Giral D, Campos-Martorell M, Garcia S, et al. A new method for focal transient cerebral ischaemia by distal compression of the middle cerebral artery. *Neuropathol Appl Neurobiol* 2012; 38: 617–27.
23. Mulle C, Sailer A, Pérez-Otano I, Dickinson-Anson H, Castillo PE, Bureau I, et al. Altered synaptic physiology and reduced susceptibility to kainate-induced seizures in GluR6-deficient mice. *Nature* 1998; 392: 601–5.
24. Nadarajan V, Perry RJ, Johnson J, Werring DJ. Transient ischaemic attacks: mimics and chameleons. *Pract Neurol* 2014; 14: 23–31.

25. Orset C, Macrez R, Young AR, Panthou D, Angles-Cano E, Maubert E, et al. Mouse model of in situ thromboembolic stroke and reper-fusion. *Stroke* 2007; 38: 2771–8.
26. Pedrono E, Durukan A, Strbian D, Marinkovic I, Shekhar S, Pitkonen M, et al. An optimized mouse model for transient ischemic attack. *J Neuropathol Exp Neurol* 2010; 69: 188–95
27. Pradhan AA, Smith ML, Zyuzin J, Charles A. μ -Opioid receptor agonists inhibit migraine-related hyperalgesia, aversive state and cortical spreading depression in mice. *Br J Pharmacol* 2014; 171: 2375–84.
28. Roose D, Leroux F, De Vocht N, Guglielmetti C, Pintelon I, Adriaensen D, et al. Multimodal imaging of micron-sized iron oxide particles following in vitro and in vivo uptake by stem cells: down to the nanometer scale. *Contrast Media Mol Imaging* 2014; 9: 400–8.
29. Rothwell PM, Coull AJ, Silver LE, Fairhead JF, Giles MF, Lovelock CE, et al. Population-based study of event-rate, incidence, case fatality, and mortality for all acute vascular events in all arterial territories (Oxford Vascular Study). *Lancet* 2005; 366: 1773–83.
30. Rothwell PM, Giles MF, Chandratheva A, Marquardt L, Geraghty O, Redgrave JN, et al. Effect of urgent treatment of transient ischaemic attack and minor stroke on early recurrent stroke (EXPRESS study): a prospective population-based sequential comparison. *Lancet* 2007 20; 370: 1432–42
31. Saleh A, Schroeter M, Jonkmanns C, Hartung HP, Mödder U, Jander S. In vivo MRI of brain inflammation in human ischaemic stroke. *Brain* 2004; 127: 1670–7.
32. Shapiro EM, Sharer K, Skrtic S, Koretsky AP. In vivo detection of single cells by MRI. *Magn Reson Med* 2006; 55: 242–9.
33. Sivakumar L, Camicioli R, Butcher K. Factors associated with cognitive decline in transient ischemic attack patients. *Can J Neurol Sci* 2014; 41: 303–13.
34. Strong K, Mathers C, Bonita R. Preventing stroke: saving lives around the world. *Lancet Neurol* 2007; 6: 182–7.
35. Touzé E, Varenne O, Chatellier G, Peyrard S, Rothwell PM, Mas JL. Risk of myocardial infarction and vascular death after transient ischaemic attack and ischemic stroke: a systematic review and meta-analysis. *Stroke* 2005; 36: 2748–55.
36. Troncoso E, Muller D, Czellar S, Zoltan Kiss J. Epicranial sensory evoked potential recordings for repeated assessment of cortical functions in mice. *J Neurosci Methods* 2000; 97: 51–8.
37. Wang X, Feuerstein GZ. Induced expression of adhesion molecules following focal brain ischemia. *J Neurotrauma* 1995; 12: 825–32.
38. Will O, Purkayastha S, Chan C, Athanasiou T, Darzi AW, Gedroyc W, Tekkis PP. Diagnostic precision of nanoparticle-enhanced MRI for lymph-node metastases: a meta-analysis. *Lancet Oncol* 2006; 7: 52–60.
39. Yang Y, Yang Y, Yanasak N, Schumacher A, Hu TC. Temporal and noninvasive monitoring of inflammatory-cell infiltration to myocardial infarction sites using micrometer-sized iron oxide particles. *Magn Reson Med* 2010; 63: 33–40.
40. Ye Q, Wu YL, Foley LM, Hitchens TK, Eytan DF, Shirwan H, et al. Longitudinal tracking of recipient macrophages in a rat chronic cardiac allograft rejection model with noninvasive magnetic resonance imaging using micrometer-sized paramagnetic iron oxide particles. *Circulation* 2008; 118: 149–56.